

PAPER

# Numerical models for ac loss calculation in large-scale applications of HTS coated conductors

To cite this article: Loïc Quéval *et al* 2016 *Supercond. Sci. Technol.* **29** 024007

View the [article online](#) for updates and enhancements.

## You may also like

- [Investigation of AC losses in horizontally parallel HTS tapes](#)  
Boyang Shen, Jing Li, Jianzhao Geng et al.
- [Transport AC losses of YBCO pancake coils wound from parallel connected tapes](#)  
V Grinenko, G Fuchs, K Nenkov et al.
- [3D modeling and simulation of 2G HTS stacks and coils](#)  
Víctor M R Zermeño and Francesco Grilli

# Numerical models for ac loss calculation in large-scale applications of HTS coated conductors

Loïc Quéval<sup>1,3</sup>, Víctor M R Zermeno<sup>2</sup> and Francesco Grilli<sup>2</sup>

<sup>1</sup> University of Applied Sciences Düsseldorf, Josef-Gockeln Strasse 9, 40474 Düsseldorf, Germany

<sup>2</sup> Karlsruhe Institute of Technology, Hermann-von-Helmholtz Platz 1, 76344 Eggenstein-Leopoldshafen, Germany

E-mail: [loic.queval@gmail.com](mailto:loic.queval@gmail.com), [victor.zermeno@kit.edu](mailto:victor.zermeno@kit.edu) and [francesco.grilli@kit.edu](mailto:francesco.grilli@kit.edu)

Received 1 June 2015, revised 13 October 2015

Accepted for publication 15 October 2015

Published 12 January 2016



## Abstract

Numerical models are powerful tools to predict the electromagnetic behavior of superconductors. In recent years, a variety of models have been successfully developed to simulate high-temperature-superconducting (HTS) coated conductor tapes. While the models work well for the simulation of individual tapes or relatively small assemblies, their direct applicability to devices involving hundreds or thousands of tapes, e.g., coils used in electrical machines, is questionable. Indeed, the simulation time and memory requirement can quickly become prohibitive. In this paper, we develop and compare two different models for simulating realistic HTS devices composed of a large number of tapes: (1) the homogenized model simulates the coil using an equivalent anisotropic homogeneous bulk with specifically developed current constraints to account for the fact that each turn carries the same current; (2) the multi-scale model parallelizes and reduces the computational problem by simulating only several individual tapes at significant positions of the coil's cross-section using appropriate boundary conditions to account for the field generated by the neighboring turns. Both methods are used to simulate a coil made of 2000 tapes, and compared against the widely used H-formulation finite-element model that includes all the tapes. Both approaches allow faster simulations of large number of HTS tapes by 1–3 orders of magnitudes, while maintaining good accuracy of the results. Both models can therefore be used to design and optimize large-scale HTS devices. This study provides key advancement with respect to previous versions of both models. The homogenized model is extended from simple stacks to large arrays of tapes. For the multi-scale model, the importance of the choice of the current distribution used to generate the background field is underlined; the error in ac loss estimation resulting from the most obvious choice of starting from a uniform current distribution is revealed.

Keywords: ac losses, numerical models, superconducting coils

(Some figures may appear in colour only in the online journal)

## 1. Introduction

The high current capacity of high-temperature-superconducting (HTS) conductors makes them ideal candidates for compact and powerful electromagnetic devices such as cables, magnets, motors, generators, and SMES. While most

of these devices are designed to operate in dc conditions, for many applications, ripple fields are expected as part of the normal operation of the device. Furthermore, several devices such as ac dipole magnets or cables are designed for working in ac conditions. As a result of these ripple and ac fields, hysteretic losses (ac losses) are expected in both transient and steady state operation. Estimating and understanding these losses is important for performance evaluation and design.

<sup>3</sup> Author to whom any correspondence should be addressed.

For a given device using HTS-coated conductor tapes, this reduces to calculating hysteretic losses of a stack or an array of tapes for at least one period. HTS material is usually modeled with a power law  $E$ - $J$  relationship that includes the dependence of  $J_c$  on the magnetic flux density and that can take overcritical current densities into consideration. This nonlinear property turns the calculation of hysteretic losses into a challenging task for devices made of hundreds or thousands of tapes since both large computing time and memory are required [1].

In this context, numerous models have been proposed to simulate large stacks and arrays of HTS coated conductors (in the references that follow, the maximum reported number of simulated tapes is indicated in curly brackets). A first group of models uses the infinitely thin-film approximation: T-formulation finite element model [2]{3}; 1D integral equations model [3]{4}. A second group of models considers the exact conductor geometry: quasi-variational inequalities formulation [4]{32}; H-formulation finite element model with large aspect ratio mapped mesh in the superconductor layer [5]{57}; minimum magnetic energy variation model assuming uniform current distribution for the tapes far from the tape of interest [6]{6400}, integral equations model assuming that the tapes far from the tape of interest can be grouped and carry a uniform current distribution [7]{12}. A third group of models uses an anisotropic homogeneous-medium approximation: [8]{n/a}, [9]{1000}, and [10]{1200} are based on the critical state model and use a predefined distribution of current in the stacks under analysis by means of either a straight line or a parabola to manually separate regions with positive, negative, or zero current density. A model that does not make any *a priori* assumptions about the current distribution in the homogenized stack is shown in [11]{100}, however, being also based on the critical state method, that work does not consider overcritical currents. A later model that does not make any *a priori* assumptions about the current distribution and that allows for overcritical local currents was presented in [12]{64}. A fourth group of models uses a multi-scale approach: first, the background field is obtained by assuming the current density in the coil windings is uniform, then the ac losses in each conductor is estimated. The estimation can either rely on measurements of single conductors [13]{2018}, or on numerical calculations [14]{2000}, [15]{40204}.

In this article, we assess and compare the ability of two different finite-element models in simulating arrays made of a large number of tapes. The first model is an extension of the homogenized model introduced in [12], which simulates the coil using equivalent anisotropic homogeneous bulks with specifically developed current constraints to account for the fact that each turn carries the same current. With respect to the original publication, the homogenized model is extended not only in terms of the number of simulated tapes (from 64 to 500), but also from simple stacks to arrays of tapes. This configuration is commonly found in large HTS magnets, composed of several pancakes positioned side-by-side. New results confirm the effectiveness of such a model in simulating large arrays of coated conductors, with reduced efforts. The second model is a multi-scale model inspired by [15].

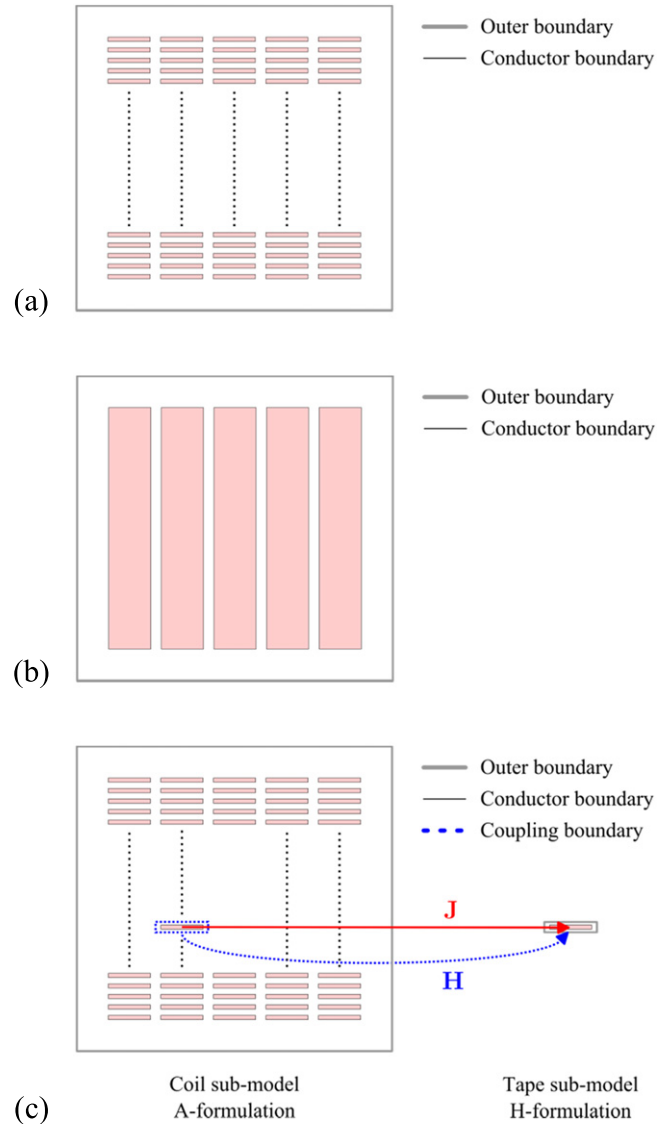


**Figure 1.** Overview of the models: (a) reference model, (b) homogenized model, (c) multi-scale model.

The main idea here is to parallelize the problem by breaking up the computational domain into several smaller domains using appropriate boundary conditions. Hence, the problem of simulating large coils reduces to simulating only one conductor at a time. This in turn reduces the memory requirement and the overall computational burden. For the first time to our knowledge, the convergence of the approach is demonstrated, and the importance of the background field in the ac losses calculation is underlined. Estimated losses and computing time are compared with the results of the established H-formulation finite element model that includes all the tapes [5]. All calculations were performed using commercial finite-element method (FEM) software [16] and a standard desktop computer (Intel i7-3770, 3.40 GHz, 4 cores, RAM 16 GB).

The article is organized as follows. In section 2, we define a test case and the reference model that will be used for validation and comparison. In section 3, we report our analysis for the homogenized model. In section 4, we perform the same study for the multi-scale model. Finally, estimated

**Table 1.** YBCO coated conductor parameters.

| Symbol       | Quantity                   | Value                                |
|--------------|----------------------------|--------------------------------------|
| $E_c$        | Critical current criterion | $1 \cdot 10^{-4} \text{ V m}^{-1}$   |
| $n$          | Power law exponent         | 38                                   |
| $J_{c0}$     | Kim model parameter        | $2.8 \cdot 10^{10} \text{ A m}^{-2}$ |
| $B_0$        | Kim model parameter        | 0.04265 T                            |
| $k$          | Kim model parameter        | 0.29515                              |
| $\alpha$     | Kim model parameter        | 0.7                                  |
| $\rho_{air}$ | Air resistivity            | 1 $\Omega\text{m}$                   |

losses, computing time, and range of application of the models are discussed and compared.

## 2. Reference model for validation

### 2.1. H-formulation

To model superconductors, we use a 2D finite element model with H-formulation [5, 17] implemented in COMSOL Multiphysics 4.3a PDE mode application. The superconductor resistivity  $\rho$  is modeled by a power law:

$$\rho(\mathbf{J}) = \frac{E_c}{J_c(\mathbf{B})} \left| \frac{\mathbf{J}}{J_c(\mathbf{B})} \right|^{n-1}, \quad (1)$$

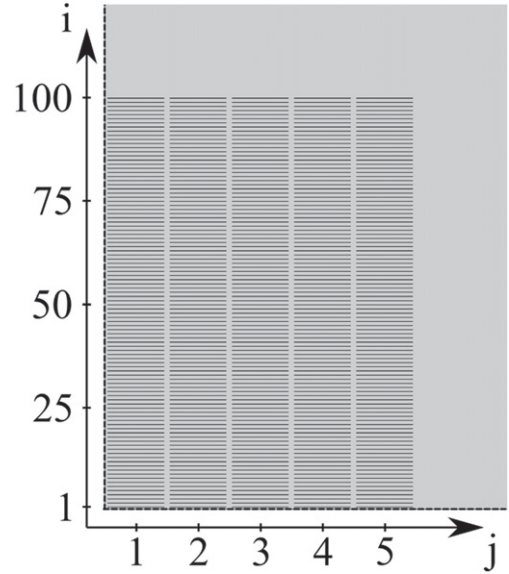
where  $J_c$  is the critical current density,  $E_c$  is the critical current criterion, and  $n$  is a material parameter. An anisotropic Kim-like model [18] is used to describe the anisotropic dependence of the critical current density on the magnetic field:

$$J_c(\mathbf{B}) = \frac{J_{c0}}{\left( 1 + \frac{\sqrt{k^2 B_x^2 + B_y^2}}{B_0} \right)^\alpha}, \quad (2)$$

where  $J_{c0}$ ,  $B_0$ ,  $k$  and  $\alpha$  are material parameters. The angle dependence of the critical current density could be easily included. Equation (2) provides a reasonable description of the anisotropic behavior of HTS coated conductors (without artificial pinning) [19]. To impose an explicit transport current in each conductor, integral constraints are used. To apply an external magnetic field, the appropriate outer boundary conditions are used. Parameters used to simulate YBCO coated conductors are summarized in table 1. They correspond to a 4 mm tape with a self-field critical current of 99.2 A [12].

### 2.2. Test case

To compare the models, we consider a large coil made of 10 pancake coils, each composed of 200 turns ( $200 \times 10$  tapes). Here, we assume 2D planar geometry, but 2D cylindrical could have been used. Due to symmetries, we can model only one-quarter of the coil ( $100 \times 5$  tapes). In the coil cross-section, the tapes have an array structure. Let their position be numbered from the bottom-left corner by two indices ( $i, j$ ). The geometric layout and tape numbering are shown in figure 2. The layout

**Figure 2.** Test case layout and tape numbering.**Table 2.** Test case layout parameters.

| Symbol | Quantity             | Value             |
|--------|----------------------|-------------------|
| a      | YBCO layer width     | 4 mm              |
| b      | YBCO layer thickness | 1 $\mu\text{m}$   |
| W      | Unit cell width      | 4.4 mm            |
| D      | Unit cell thickness  | 293 $\mu\text{m}$ |

parameters are summarized in table 2. We study the case of transport current (no applied external field), and we impose ac transport currents at 50 Hz with amplitudes of 11 A and 28 A. 11 A is the amplitude at which the central tapes in the outermost column ( $i = 1, j = 5$ ) have no virgin regions. This is to say they are filled with either transport or magnetization currents. 28 A is the current at which the central tapes in the outermost column ( $i = 1, j = 5$ ) are fully penetrated with transport currents, which means the magnetization currents have been displaced in these tapes. We define this later value as the critical current of the coil since any additional current would imply substantially exceeding the critical current density in at least one tape. We simulate the model for one period and use the second half of this period to compute the average power loss per cycle (in  $\text{W m}^{-1}$ ) using:

$$P = \frac{2}{T} \int_{T/2}^T dt \int_{\Omega} \mathbf{E} \cdot \mathbf{J} d\Omega, \quad (3)$$

where  $T$  is the period of the cycle and  $\Omega$  is the superconductor domain.

### 2.3. Reference model

The reference model is an H-formulation model including all the tapes (figure 1(a)). H-formulation models have been widely used and verified against experiments for single conductors and coils [20–27] and can therefore be trusted to give a good estimation of the real losses. Besides the surrounding

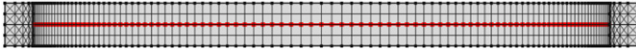


**Figure 3.** Unit tape cell mesh. The red line represents the superconductor layer.

air, we model only the superconducting layers, taking their real thickness into account. To mesh the superconducting layer, we used a mapped mesh [5] with 100 elements distributed symmetrically following an arithmetic sequence in the width and 1 element in the thickness. We also used a mapped mesh between the tapes. The mesh of one unit cell of the array is shown in figure 3.

### 2.4. Results

The normalized current density distribution and the magnetic flux density distribution at  $t = 0.015$  s (peak current) for the 11 A transport current case are shown in figure 4; the tape thickness was artificially expanded in the vertical direction for visualization. The magnetic-field distribution observed is due to the magnetization currents, which tend to prevent the field to penetrate the tapes. This effect is particularly strong at low transport currents. The hysteretic losses for each tape are plotted in figure 7. In a given row  $i$ , the losses spread out across almost three orders of magnitude. But in a given column  $j$ , the losses are similar.

## 3. Homogenized model

### 3.1. Modeling strategy

The homogenized model was introduced in [12] for modeling 2D stacks of HTS coated conductors (up to 64 tapes). In [28],

it was adapted to 3D racetrack coils (50 turns). In comparison to other homogenized models [8–11], this model does not make any *a priori* assumptions about the current distribution and allows for overcritical local currents. In this article, we extend it to simulate large arrays of tapes. The homogenized model simulates the coil using equivalent anisotropic homogeneous bulks (figure 1(b)) with specifically developed current constraints to account for the fact that each turn carries the same current. This allows us to take advantage of the vanishing edge effect toward the center of the stack ( $i = 1$ ) and to use a very coarse mesh (figure 6), thus reducing the computing time. For modeling details, we refer the reader to [12].

### 3.2. Results

To provide a qualitative comparison between the reference model and the homogenized model, the 11 A transport current case is analyzed. The normalized current density distribution and the magnetic flux density distribution at  $t = 0.015$  s (peak current) are shown in figure 5. The distributions calculated with the homogenized model reproduce overall well the reference model. The field distribution in each stack is smoother because the homogenization washes out the actual tapes layout. The hysteretic losses for each tape are plotted in figure 7. For both transport current cases, the error between the losses estimated with the homogenized model and the reference model is less than 1% (table 3), for a speed up factor of 50–70 (table 4).

### 3.3. Discussion

The step-like shape of the ‘homogenization’ curve is due to the mesh (figure 6): the mesh is coarse at the center of each stack ( $i = 1$ ) where the spatial variation of the magnetic field

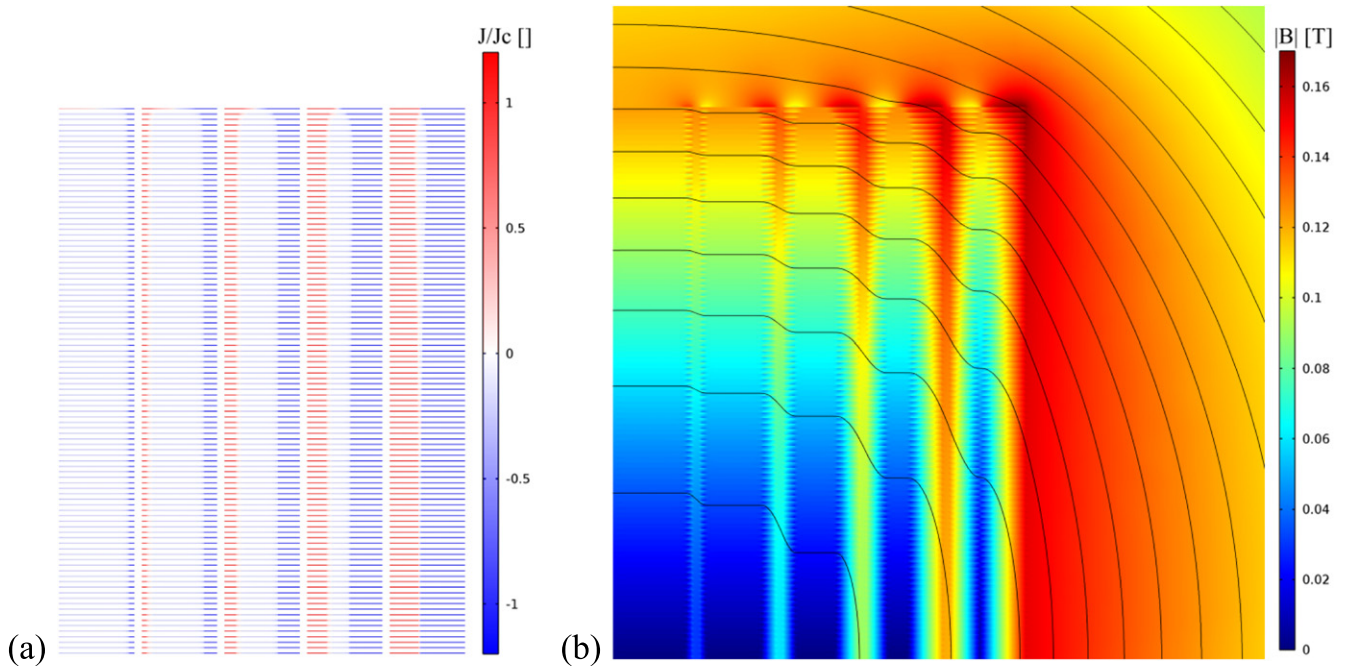


**Figure 4.** Reference model (a) normalized current density distribution, (b) magnetic flux density distribution (11 A,  $t = 0.015$  s).



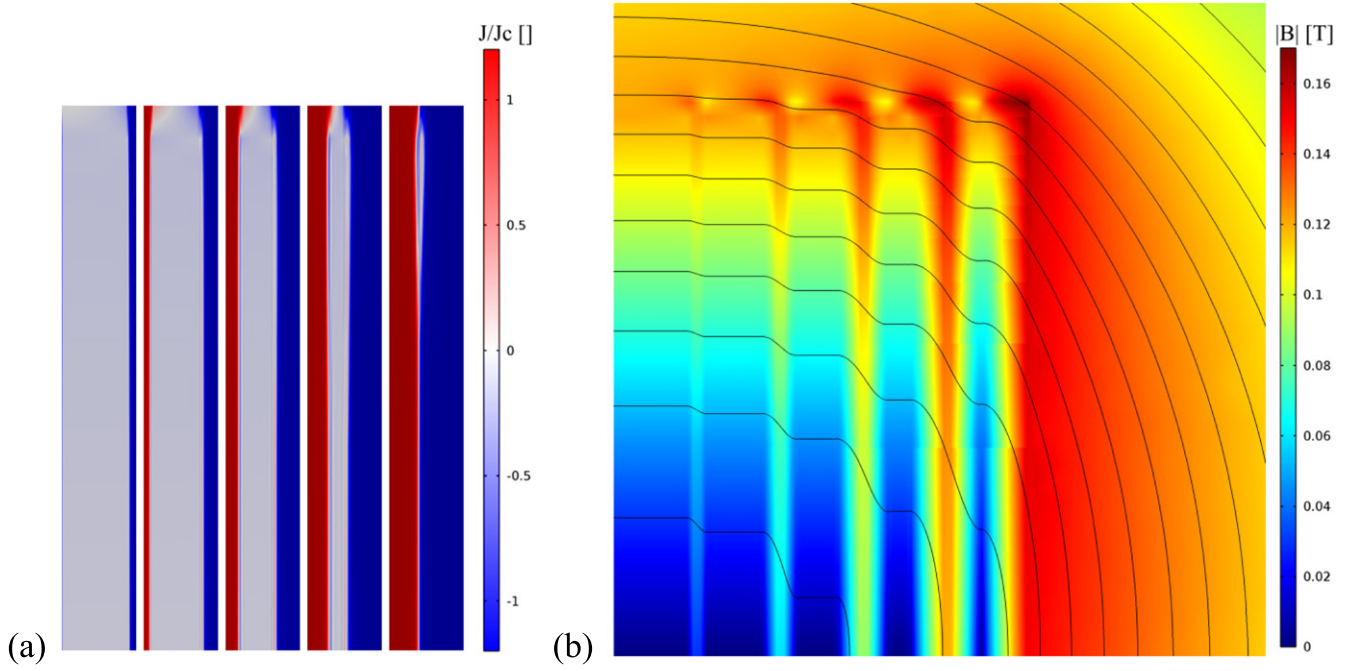


**Figure 5.** Homogenized model (a) normalized current density distribution, (b) magnetic flux density distribution (11 A,  $t = 0.015$  s).

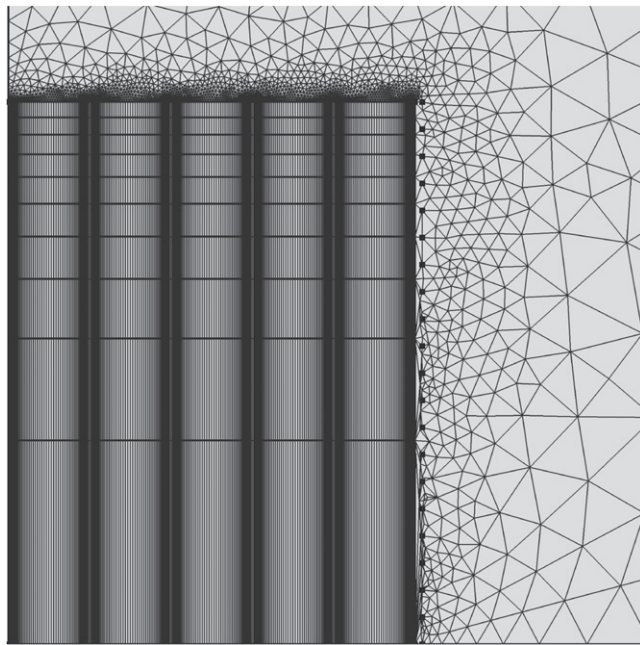


**Figure 6.** Homogenized model mesh. Each stack is meshed with 10 elements distributed logarithmically along the height, and 50 elements distributed symmetrically following an arithmetic sequence along the width.

is small and finer toward the top of each stack ( $i = 100$ ) to have enough spatial resolution to model the end effects. The coarse mesh helps reduce the number of degrees of freedom (table 5), and thus the computing time. Locally, the estimated losses closely follow the ones given by the reference model. For the first stack ( $j = 1$ ), the model slightly overestimates them (figure 7). However, this is of little consequence to our overall estimation. We note the close match for the local

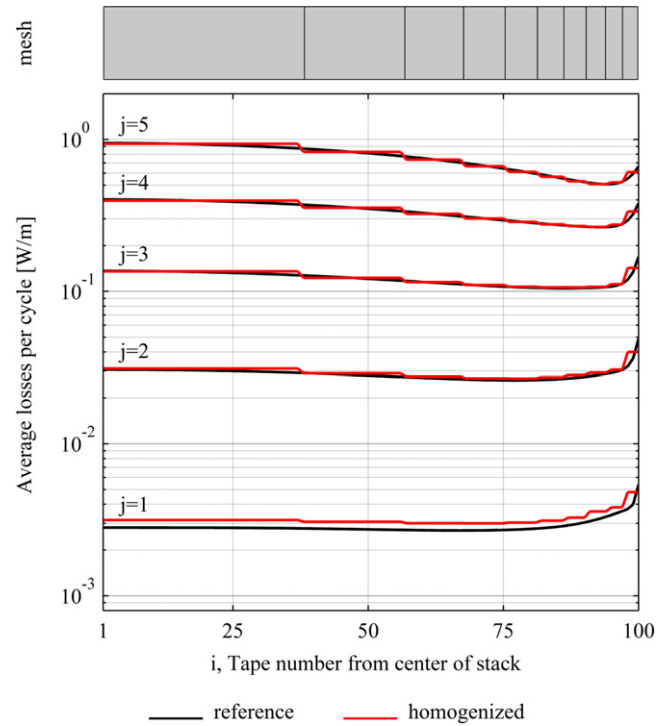


**Figure 7.** Homogenized model hysteretic losses for the 11 A transport current case. ( $i, j$ ) is the tape numbering in the array (see figure 2). The step-like behavior of the losses is linked to the mesh structure across the height of the stacks as shown above the graph.

losses estimation across the whole coil. This is not trivial since these values span across almost three orders of magnitude. The simple implementation of the homogenized model in a commercial finite-element program is a clear advantage. In addition to its good ability in predicting hysteretic losses, it also proved to be stable. However, the homogenized model is

**Table 3.** Hysteretic Losses.

| Model                               | Losses [ $\text{W m}^{-1}$ ] | Losses [ $\text{W m}^{-1}$ ] |
|-------------------------------------|------------------------------|------------------------------|
|                                     | 11 A transport current       | 28 A transport current       |
| Reference                           | 127.02                       | 933.99                       |
| Homogenized                         | 127.92 (100.7%)              | 934.41 (100.0%)              |
| Multi-scale $J_0$<br>uniform        | 96.46 (75.9%)                | 909.06 (97.3%)               |
| Multi-scale $J_0$<br>infinite array | 119.85 (94.4%)               | 917.57 (98.2%)               |

**Table 4.** Computing time.

| Model                               |                            | Time [h]               | Time [h]               |
|-------------------------------------|----------------------------|------------------------|------------------------|
|                                     |                            | 11 A transport current | 28 A transport current |
| Reference                           |                            | 21.3                   | 52.0                   |
| Homogenized                         |                            | 0.3                    | 1.1                    |
| Multi-scale $J_0$<br>uniform        | Series <sup>a</sup>        | 0.3                    | 0.7                    |
|                                     | Parallel <sup>b</sup>      | 0.08                   | 0.15                   |
|                                     | Full parallel <sup>c</sup> | 0.03                   | 0.04                   |
| Multi-scale $J_0$<br>infinite array | Series <sup>a</sup>        | 0.9                    | 1.4                    |
|                                     | Parallel <sup>b</sup>      | 0.4                    | 0.6                    |
|                                     | Full parallel <sup>c</sup> | 0.3                    | 0.4                    |

<sup>a</sup> series computation (1 core), calculated on PC (Intel i7-3770, 3.40 GHz, 4 cores, RAM 16 GB).

<sup>b</sup> parallel computation (5 cores), estimated.

<sup>c</sup> full parallel computation (25 cores), estimated.

**Table 5.** Degrees of freedom.

| Model                    | DOF    |
|--------------------------|--------|
| Reference                | 606276 |
| Homogenized              | 14512  |
| Multi-scale <sup>a</sup> | 1415   |

<sup>a</sup> Multi-scale model tape submodel.

limited to tape-like conductors with thin superconducting layer. Indeed, in principle the model is equivalent to a stack of infinitely thin tapes and cannot take into account the magnetization currents due to a magnetic field parallel to the wide surface of the tape. Furthermore, the homogenization method, at its current stage, cannot include magnetic materials. Thus, it is not applicable to Bi-2223 tapes, Bi-2212, or  $\text{MgB}_2$  wires.

## 4. Multi-scale model

### 4.1. Modeling strategy

The multi-scale model was introduced in [15] to estimate the steady state ac losses of a superconducting wind turbine

generator connected to the grid through its ac/dc/ac converter ( $1058 \times 38$  tapes). In this work, we extend it by (a) adding the magnetic field dependence of the critical current density and (b) introducing a refined background field estimation. This last point permits including partially the fact that the other tapes are superconducting. The analysis reported here also serves as validation, since the agreement with the reference model has thus far been unclear. The main idea behind the multi-scale model is to (1) estimate the background field using a fast coil model, and (2) calculate the ac losses of only several tapes at significant positions of the coil's cross-section using this local field. The losses of the other tapes are then obtained by interpolation. By breaking up the coil domain into several smaller subdomains, we can parallelize the problem and thus reduce its computation time. The multi-scale model is composed of two submodels (figure 1(c)). The coil submodel is a conventional A-formulation magnetostatic finite-element model. It includes all the tapes with their actual geometry, and assumes a given current density distribution  $J_0$  (uniform or not). The tape submodel is an H-formulation finite-element model, which includes only one conductor with its actual geometry. The coupling between the two submodels is unidirectional. The magnetic field strength  $H$  obtained with the coil submodel is exported along a coupling boundary lying along the unit cell boundary. It is then applied to the tape submodel as a time-varying Dirichlet boundary condition. An integral constraint is used to impose the total transport current in the conductor. The meshes used for both multi-scale submodels are similar to those of the reference model.

### 4.2. Results

We first analyze the 11 A transport current case. The purpose of the coil submodel is to obtain a good picture of the local background field to be applied to the tape submodel.

- $J_0$  uniform:* In a first approximation, we can consider that  $J_0$  is uniform over the tape's cross-section (figure 8(a)). This is the standard approach [14, 15].  $J_0$  is simply obtained by dividing the coil transport current by the tape cross-section. The resulting magnetic flux density distribution at  $t = 0.015$  s is shown in figure 8(b). The distributions poorly reproduce the ones of the reference model (figure 4). As a result, the hysteretic losses are underestimated (figure 10 and table 3). However, the speed up factor of up to 700 (table 4), decreasing the total computing time to less than 90 s, might make this model of interest for preliminary design and optimization.
- $J_0$  infinite array:* In reality, the local magnetic field of one HTS tape in a coil depends on the current distribution of the adjacent tapes (both transport and magnetization currents, which are unknown). In an attempt to include this effect, we propose approximating  $J_0$  as the current density distribution of an infinite array of five tapes ( $i = \infty$ ,  $j = 5$ ) (figure 9(a)).  $J_0$  is obtained by simulating only five tapes side-by-side with appropriate periodic boundary conditions and a coarse mesh. The resulting magnetic flux density distribution at  $t = 0.015$  s is shown in figure 9(b). The distributions

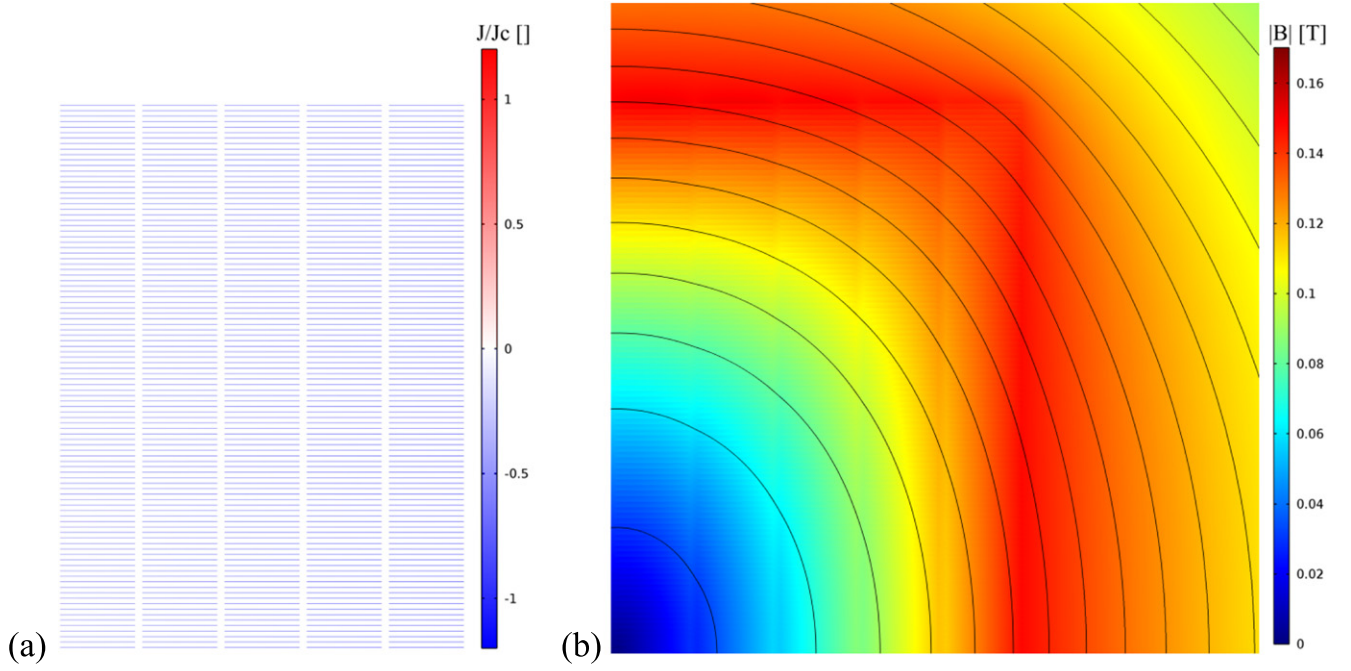


**Figure 8.** Multi-scale coil submodel with  $J_0$  uniform (a) normalized current density distribution, (b) magnetic flux density distribution (11 A,  $t = 0.015$  s).

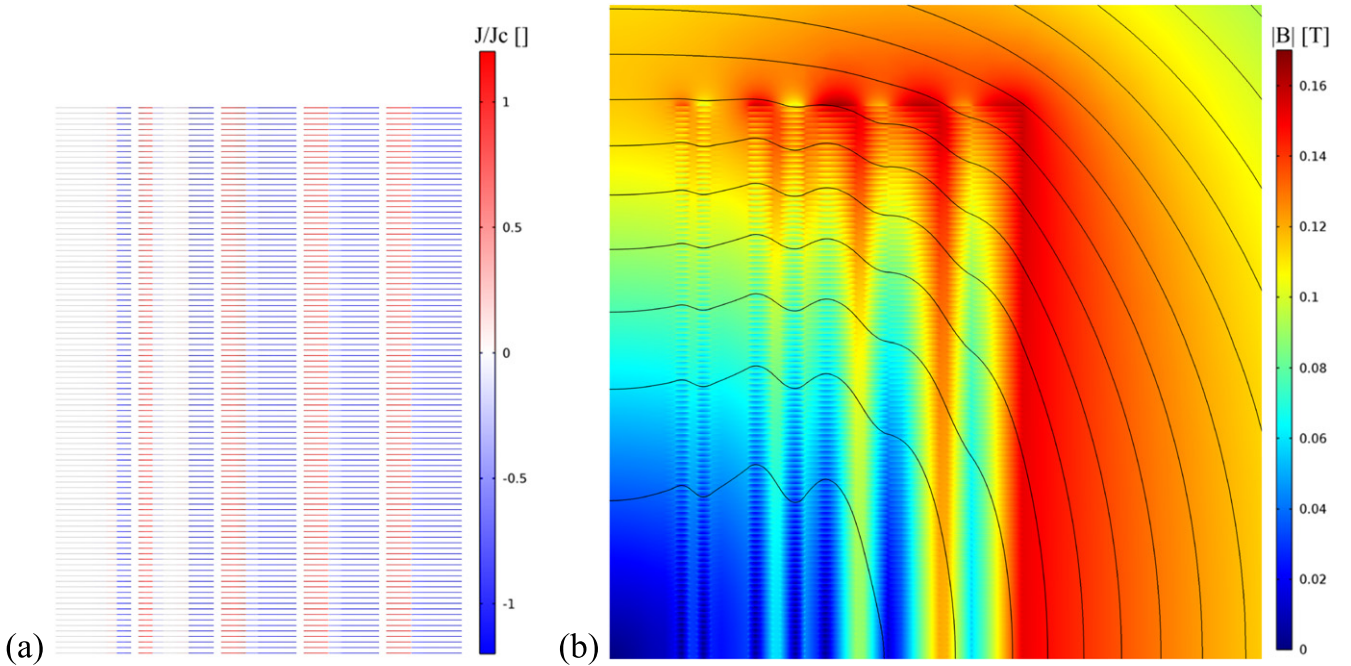


**Figure 9.** Multi-scale coil sub-model with  $J_0$  'infinite array' (a) normalized current density distribution, (b) magnetic flux density distribution (11 A,  $t = 0.015$  s).

now better reproduce those of the reference model (figure 4), especially in the coil center where the infinite array is a good approximation. As expected, the hysteretic losses are in better agreement with the ones obtained from the reference model (figure 10 and table 3). An error of 6% is considered small bearing in mind that the value of the losses in the tapes spreads almost three orders of magnitude. However, the

preliminary computation of  $J_0$  has a cost, both in terms of implementation and computation time (table 4).

(c)  $J_0$  reference model: This case has no practical application but demonstrates the convergence of the method. If  $J_0$  is taken as the current density distribution of the reference model (figure 4(a)), the hysteretic losses are accurately predicted (figure 10). Therefore, the accuracy of the multi-scale model is only limited by



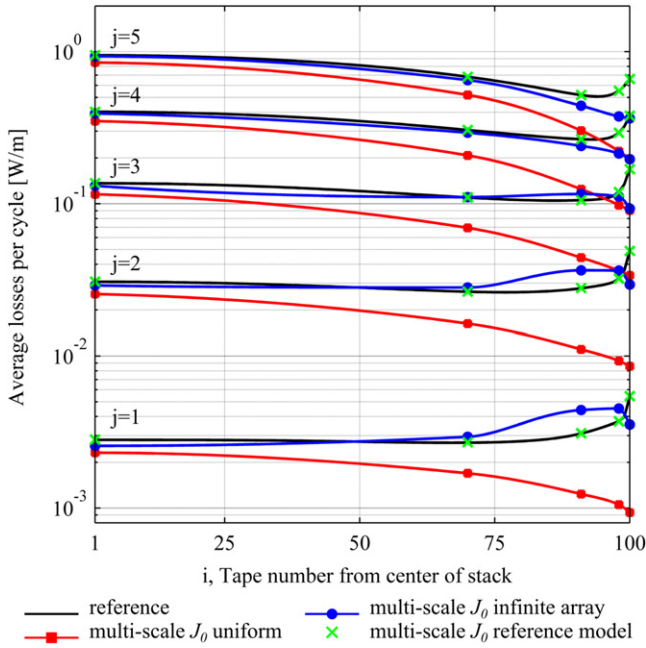


**Figure 10.** Multi-scale model hysteretic losses for the 11 A transport current case. The markers show the calculated tapes. Losses for the other tapes are obtained by interpolation.  $(i, j)$  is the tape numbering in the array (see figure 2).

the poor estimation of the background field when using  $J_0$  uniform or  $J_0$  infinite array.

In the 28 A transport current case, the multi-scale model with  $J_0$  uniform is able to predict the losses with a good accuracy (table 3) for a speed up factor of up to 1600 (table 4). This can be explained by looking at reference model at  $t = 0.015$  s (figure 11): the normalized current

distribution is almost uniform and produces a field similar to the one of the multi-scale coil submodel with  $J_0$  uniform (figure 8(b)).

#### 4.3. Discussion

We calculate only several tapes and interpolate the results to the other tapes. The choice of the tapes is similar to the choice of a mesh. We need more tapes in regions where the field spatial variation is higher. Here it is sufficient to take five tapes distributed logarithmically over each stack: the difference with the losses obtained by calculating all the tapes is  $\sim 1\%$  (not reported here). The main advantages of the multi-scale model are the low memory requirement (table 5) and the possibility to simulate every tape submodel in parallel. The computing time in table 4 is given for series computation (1 core), parallel computation (five cores, e.g., desktop workstation), and full parallel computation (5 cores, i.e., 1 core per tape with dedicated hardware). With  $J_0$  uniform, we need only a static multi-scale coil submodel. With  $J_0$  infinite array, a transient coil submodel is required, in addition to the preliminary calculation of  $J_0$ . This explains the difference in computing time in table 4. For example, for the 11 A transport current case, the computing time for the multi-scale model with  $J_0$  uniform was 28 s for the coil submodel (static), 18 s for export, and 45 s in average per tape submodel. With  $J_0$  infinite array, the computing time was 310 s for the infinite array (transient), 554 s for the coil submodel (transient), 169 s for export, and 87 s in average per tape submodel. Analytical expressions may be of interest here to estimate  $J_0$  and to further reduce computing time. We note that, in comparison to the homogenized model, the multi-scale model could be applied to any kind of conductor, including multifilamentary  $\text{MgB}_2$ , Bi-2223, and Bi-2212 tapes or wires and coated

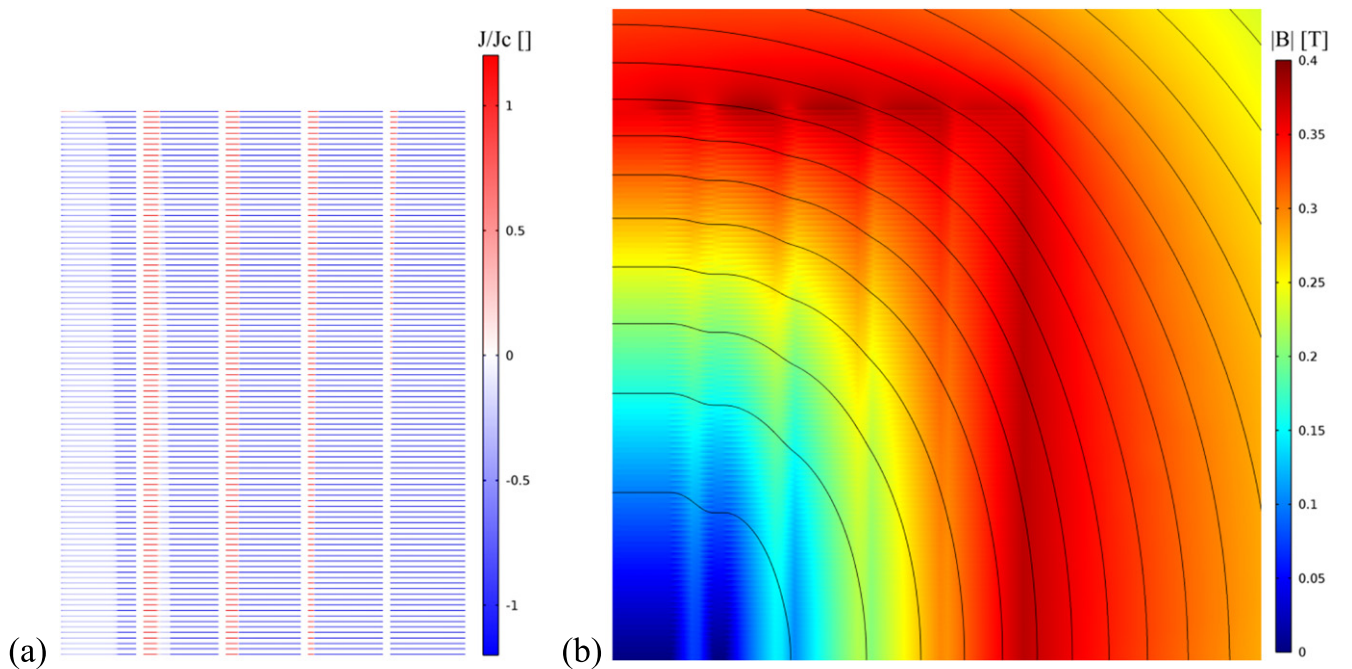


**Figure 11.** Reference model (a) normalized current density distribution, (b) magnetic flux density distribution (28 A,  $t = 0.015$  s).

conductor tapes with magnetic substrate. On the one hand, the implementation time of the tape submodel is low because we need to model only one tape. However, on the other hand the coupling between the coil submodel and the tape submodel could not be performed directly via COMSOL Multiphysics interface, and required data processing between exporting and importing the coupling boundary field.

## 5. Conclusion

The motivation behind this work was to develop reliable and fast numerical models to simulate devices wound of hundreds—or even thousands—of HTS coated conductors. Since at least one ac cycle needs to be simulated in order to estimate superconductor ac losses, simulating all the tapes is not an option. We have therefore developed two complementary approaches: the homogenized model and the multi-scale model.

The homogenized model was extended with respect to its original version for simple stacks, and the possibility of simulating large arrays of tapes has been validated. For the first time to our knowledge, the accuracy and convergence of the multi-scale approach was compared against a reference case. It was proven that the assumption of uniform current distribution in the multi-scale approach can lead to a severe (and potentially dangerous) underestimation of the ac losses. In addition, the accuracy and speed of the multi-scale approach was tested against a competing approach (homogenization).

In terms of computational performance, the homogenized model is fast, it provides the best ac losses estimation, and it is much easier to set up than the reference model. Being 50–70 times faster than the reference model it provides a good cost-benefit once computing and setup times are considered. Moreover, we could further reduce its computing time at the sacrifice of accuracy by using a coarser mesh. On the other hand, it only works for coated conductor tapes without magnetic substrate. However, this is not considered to be a great disadvantage considering that today most coated conductor tapes are manufactured deposited on non-magnetic substrates.

The multi-scale model is the fastest, especially if we consider the advantage of parallelization. The use of a coil submodel with  $J_0$  uniform enables low computing time, but it comes at the price of larger error, especially for low current amplitude. By improving the quality of the background field (coil submodel with  $J_0$  infinite array), we can reduce the error. But this leads to longer computing time, and relies on the availability of a fast method to approximate the background field for the given problem. In general, this model provides a good tradeoff between computing time, number of processors, and memory requirements. In addition, it is flexible for design and optimization: once the regions of the coil that contribute the most to the losses are identified, we can study only those regions without the need to compute the whole coil every time. It can in principle be used for any kind of conductor, including multi-filamentary tapes or tapes with magnetic

materials. It is also easier to set up than the reference model. Finally for extremely large coils, this might be the only method due to the parallel capability.

Both models allow drastic computing time reduction while keeping estimated ac losses in good agreement with those calculated simulating the entire device. Such models could be used to design and optimize large-scale HTS devices.

## References

- [1] Sirois F and Grilli F 2015 Potential and limits of numerical modelling for supporting the development of HTS devices *Supercond. Sci. Technol.* **28** 043002
- [2] Ichiki Y and Ohsaki H 2005 Numerical analysis of ac loss characteristics of YBCO coated conductors arranged in parallel *IEEE Trans. Appl. Supercond.* **15** 2851–4
- [3] Brambilla R, Grilli F, Nguyen D N, Martini L and Sirois F 2009 Ac losses in thin superconductors: the integral equation method applied to stacks and windings *Supercond. Sci. Technol.* **22** 075018
- [4] Šouc J, Pardo E, Vojenčiak M and Gömöry F 2009 Theoretical and experimental study of ac loss in high temperature superconductor single pancake coils *Supercond. Sci. Technol.* **22** 015006
- [5] Zermeno V M R, Mijatovic N, Traeholt C, Zirngibl T, Seiler E, Abrahamsen A B, Pedersen N F and Sørensen M P 2011 Towards faster FEM simulation of thin film superconductors: a multiscale approach *IEEE Trans. Appl. Supercond.* **21** 3273–6
- [6] Pardo E 2014 Calculation of ac loss in coated conductor coils with a large number of turns *Supercond. Sci. Technol.* **26** 5017
- [7] Carlier M 2012 Modèle intégral axisymétrique pour le calcul des pertes AC dans les bobinages supraconducteurs *MSc Thesis École Polytechnique de Montréal* (in French)
- [8] Clem J R, Claassen J H and Mawatari Y 2007 Ac losses in a finite Z stack using an anisotropic homogeneous-medium approximation *Supercond. Sci. Technol.* **20** 1130–9
- [9] Yuan W, Campbell A M and Coombs T A 2009 A model for calculating the ac losses of second-generation high temperature superconductor pancake coils *Supercond. Sci. Technol.* **22** 075028
- [10] Zhang H, Zhang M and Yuan W 2015 Ac loss calculation for multi pancakes of (Re)BCO coated conductor using line front arXiv:1406.5869
- [11] Prigozhin L and Sokolovsky V 2011 Computing ac losses in stacks of high-temperature superconducting tapes *Supercond. Sci. Technol.* **24** 075012
- [12] Zermeno V M R, Abrahamsen A B, Mijatovic N, Jensen B B and Sørensen M P 2013 Calculation of alternating current losses in stacks and coils made of second generation high temperature superconducting tapes for large scale applications *J. Appl. Phys.* **114** 173901
- [13] Oomen M P, Nanke R and Leghissa M 2003 Modelling and measurement of ac loss in BSCCO/Ag-tape windings *Supercond. Sci. Technol.* **16** 339
- [14] Tonsho H, Toyoda M, Fukui S, Yamaguchi M, Sato T, Furuse M, Tanaka H, Arai K and Umeda M 2004 Numerical evaluation of ac loss in high temperature superconducting coil *IEEE Trans. Appl. Supercond.* **14** 674–7
- [15] Quéval L and Ohsaki H 2013 AC losses of a grid-connected superconducting wind turbine generator *IEEE Trans. Appl. Supercond.* **23** 5201905
- [16] 'COMSOL Multiphysics version 4.3a' Available: [www.comsol.com](http://www.comsol.com)

- [17] Brambilla R, Grilli F and Martini L 2007 Development of an edge-element model for ac loss computation of high-temperature superconductors *Supercond. Sci. Technol.* **20** 16–24
- [18] Kim Y B, Hempstead C F and Strnad A R 1962 Critical persistent currents in hard superconductors *Phys. Rev. Lett.* **9** 306
- [19] Grilli F, Sirois F, Zerméño V M R and Vojenčiak M 2014 Self-consistent modeling of the  $I_c$  of HTS devices: how accurate do models really need to be? *IEEE Trans. Appl. Supercond.* **24** 1–8
- [20] Grilli F and Ashworth S P 2007 Measuring transport ac losses in YBCO-coated conductor coils *Supercond. Sci. Technol.* **20** 794–9
- [21] Grilli F, Brambilla R and Martini L 2007 Modeling high-temperature superconducting tapes by means of edge finite elements *IEEE Trans. Appl. Supercond.* **17** 3155–458
- [22] Nguyen D N, Grilli F, Ashworth S P and Willis J O 2009 Ac loss study of antiparallel connected YBCO coated conductors *Supercond. Sci. Technol.* **22** 055014
- [23] Nguyen D N, Ashworth S P, Willis J O, Sirois F and Grilli F 2010 A new finite-element method simulation model for computing ac loss in roll assisted biaxially textured substrate YBCO tapes *Supercond. Sci. Technol.* **23** 025001
- [24] Zhang M, Kim J-H, Pamidi S, Chudy M, Yuan W and Coombs T A 2012 Study of second generation, high-temperature superconducting coils: determination of critical current *J. Appl. Phys.* **111** 39021–8
- [25] Wang W and Coombs T 2015 The magnetisation profiles and ac magnetisation losses in a single layer YBCO thin film caused by travelling magnetic field waves *Supercond. Sci. Technol.* **28** 055003
- [26] Celebi S, Sirois F and Lacroix C 2015 Collapse of the magnetization by the application of crossed magnetic fields: observations in a commercial Bi:2223/Ag tape and comparison with numerical computations *Supercond. Sci. Technol.* **28** 025012
- [27] Zerméño V M R, Grilli F and Sirois F 2013 A full 3D time-dependent electromagnetic model for Roebel cables *Supercond. Sci. Technol.* **26** 052001
- [28] Zerméño V M R and Grilli F 2014 3D modeling and simulation of 2G HTS stacks and coils *Supercond. Sci. Technol.* **27** 4025